Article:
Faramehr, S., Poluri, N., Igic, P. et al. (2019) Development of GaN transducer and on-chip concentrator for galvanic current sensing. IEEE Transactions on Electron Devices, 66 (10). pp. 4367-4372. ISSN: 0018-9383

https://doi.org/10.1109/ted.2019.2936687

Development of GaN Transducer and On-chip Concentrator for Galvanic Current Sensing

Soroush Faramehr, Nagaditya Poluri, Petar Igić, Nebojsa Janković and Maria Merlyne De Souza

***Abstract*— Gallium nitride (GaN) magnetic high electron mobility transistors (MagHEMTs) with different gate lengths intended for integration with magnetic flux concentrator for galvanic isolation are presented. Detailed discussions on the physical mechanisms behind the sensitivity change at room temperature with respect to gate geometry are given. The relative sensitivity of dual-drain GaN MagHEMTs with device length of L=65 µm and width of W=20 µm are measured at the highest of S=17.21 %/T and lowest of S=7.69 %/T at V_{GS}=–2V and V_{GS}=0V, respectively. In addition, a novel spiral magnetic flux concentrator with the conversion factor of up to F_C=96 mT/A is designed for improving the performance of the optimised MagHEMTs in ICs. It is predicted that a spiral configuration is a necessity to enhance the conversion factor for a long MagHEMT.**

***Index Terms*— GaN, MagHEMTs, Concentrator.**

I. Introduction

Compact and accurate current sensing is a major step toward wide bandgap power conversion systems. A significant improvement in terms of bandwidth, performance and accuracy has been achieved in Hall-effect, Rogowski and magnetoresistive sensors over the last few years [1].

The most common approaches for current sensing are shunt resistor and Faraday induction-based. Shunt resistor-based sensing comes with power loss, frequency dependent parastitics and no galvanic isolation [2]. Faraday induction provides the galvanic isolation and enhanced frequency properties but filters DC and possesses bulky, costly and loss-prone core [3] that cannot be integrated into power modules. Rogowski coil can be integrated into power modules but the intricate coil design and the integrator makes it expensive, complex and prone to errors [2], [3], [4].

Magnetoresistive and Hall-effect sensors, both compatible with IC technologies, are commonly utilised to detect magnetic fields. While magnetoresistive phenomenon works on the basis of act of magnetic field on the spin of electrons, the hall-effect phenomenon operates on the basis of act of magnetic field on the charge of electrons. The choice of technology is heavily dependent on the target application with the Hall-effect being the one with linearity in a wide range of magnetic fields from nano-Tesla to several tens of Tesla [5].

Mangnetic field-based current sensing measures the current using the Maxwell-Ampere's law to provide the galvanic isolation needed in power applications. The generated field is from either power load or the SenseFET current. This approach increases efficiency, reduces circuit cost and provides a wide bandwidth.

Galvanic isolation can be provided by magnetic sensitive field effect transistor (MagFET). The MagFET utilizes the Lorentz force principle [6], [7] in the presence of a magnetic field focused and amplified by a magnetic flux concentrator.

The advantages of a gallium nitride (GaN) heterostructure over conventional semiconductors make it a promising replacement for silicon-based Hall-effect devices in RF and power applications [8], [9]. Recently, we have demonstrated superior performance of the GaN sensors (ungated) at elevated temperatures [10] surpassing silicon counterparts [11]. In addition, silicon based Hall-effect sensors have a limited bandwidth of a few KHz, compound semiconductors including gallium arsenide and indium arsenide have enabled a detection bandwidth of tens of MHz [1].

The GaN current sensors, hereafter referred to as magnetic sensitive high electron mobility transistors (MagHEMTs), takes advantage of the properties of the two-dimensional electron gas (2DEG) including high electron mobility and nano-meter range thickness [12] formed at an $Al_xGa_{1-x}N$/GaN interface.

Sheet and tip flux concentrators that bend and concentrate the field, respectively require fabrication steps at the back of the substrate, including substrate thinning. In contrast, integrated magnetic concentrators (referred as IMCs) are integrated on the same side as the sensor [13]. IMCs utilize the fringing magnetic field and have demonstrated an increase in strength of the magnetic field by ×21 [14]. However, these require a large chip space several orders of magnitude larger than the sensor in order to achieve field uniformity in the normal direction.

In this paper we report on 1st ever fabricated dual-drain GaN MagHEMT current sensors. The transfer (I_D-V_{GS}) characteristics and sensitivity values are given at different biasing conditions and the effect of gate length on the sensitivity is investigated at room temperature. In addition, since the MagHEMTs fabricated possess long channels to enhance the Hall geometrical correction factor (G_H), a single loop flux concentrator we had previosuly demonstrated [15] is modified and a novel spiral magnetic flux concentrator in closest approximity to the sensor to improve the conversion factor for long MagHEMTs is examined.

Manuscript received on May xx, 2019. This work was supported by EPSRC as CN/FEAS17/ITSIA project.

Soroush Faramehr and Petar Igić are with the Centre for Advanced Low-carbon Propulsion Systems (C-ALPS), Institute for Future Transport and Cities, Coventry University, Coventry CV1 5FB U.K. (e-mail: ad2057@coventry.ac.uk and ad1503@coventry.ac.uk).

Nagaditya Poluri and Maria Merlyne De Souza are with the Department of Electrical and Electronics Engineering, University of Sheffield, Sheffield S37HQ, U.K. (e-mail: npoluri1@sheffield.ac.uk and m.desouza@sheffield.ac.uk).

Nebojsa Janković is with the Faculty of Electronic Engineering, University of Nis, 18000 Nis, Serbia. (e-mail: nebojsa.jankovic@elfak.ni.ac.rs).

II. GaN MagHEMT Fabrication and Characterisation

Figure 1 (a) is the schematic of the GaN MagHEMTs with its magnetic field components resulting from magnetic concentration and Figure 1 (b) is the micro-photograph of a fabricated device.

In rectangular split-drain current sensors operating in the linear mode, the current difference between the two drains is called Hall current ($\mathbf{I}_H$) and is expressed by [16]:

$$I_H = \mu_H B_z (L/W) I_D G_H \quad (1)$$

where μ_H is Hall mobility, B_z is applied magnetic field in z-direction (perpendicular to device surface), L is device length, W is device width, I_D is output current and G_H is Hall geometrical correction factor, a ratio of Hall voltage in a real Hall plate to ideal (infinite) Hall plate [17].

The current imbalance of the MagHEMT can be measured on split contacts and its sensitivity (S) is calculated similar to previously reported in literature for MagFETs by the following expression [10]:

$$S = \frac{|I_{D1}-I_{D2}|-I_{offset}}{(I_{D1}+I_{D2})|B|} \times 100\% \quad (2)$$

where I_{D1} and I_{D2} are the currents from drain 1 and drain 2 respectively, in the presence of magnetic field ($\boldsymbol{B}$), and I_{offset} is the current difference in the absence of a magnetic field.

The unintentionally doped (UID) gated sensors are GaN/$Al_xGa_{1-x}N$/GaN heterostructures with step-graded AlGaN intermediate layers on silicon substrate with the mole fraction of x=0.25. The GaN cap, AlGaN barrier, and GaN buffer thicknesses are 2 nm, 25 nm and 1.8 µm, respectively. Mesas are created to define device active regions on 6-inch GaN wafer using dry etching process in inductively coupled plasma (ICP) system. Ti/Al/Ti/Au metal stacks for source and drain contacts are deposited with physical vapor deposition (PVD). The stacks are subsequently annealed at 800 °C in a rapid thermal annealing (RTA) system with N_2 ambient to form the Ohmic contacts. Schottky Ni/Au gate contacts are deposited by PVD. Finally, SiN passivation is deposited using plasma enhanced chemical vapor deposition (PECVD) followed by contact opening process.

Figure 2 shows transfer characteristics of a GaN MagHEMT with gate length of L_G=5 µm, device length of L=65 µm and width of W=20 µm. The output currents from the two drains are plotted against input voltage (V_{GS}) demonstrating the current offset between the two drains in the absence of magnetic field.

The offset is increased from I_{offset}=1.1×10^{-6} A at V_{GS}=0V and V_{DS}=0.1V to I_{offset}=1.03×10^{-5} A for the higher drain bias of V_{DS}=1V. A narrower contact increases the current density as reported in [17]. The current measured at drain 1 is consistently larger than the one measured at drain 2 for various drain biasing conditions. The effect is more pronounced at larger biases due to increase (reduction) in electric field at the contact with smaller (larger) width since both electrodes are biased with the same potential.

The offset observed in Hall sensors is undesirable limiting their ability to discriminate small steady-state magnetic fields [16]. The offset is assigned to multiple factors such as alignment error in contacts and material inhomogeneities [16]. Consequently, there has been significant investigation on this downside. Therefore, once confined to lower end magnetic measurements, now Hall sensors are more suitable for applications with micro-Tesla and even nano-Tesla range requirement [18].

Figure 3 is the current imbalance (ΔI) induced in the dual drain GaN MagHEMT and its ratio to the total current (ΣI=I_{D1}+I_{D2}). The deflected current follows the same trend as transfer characteristics against input voltage. Analogous to the output current, at higher gate voltages (close to 0V), the Hall current has a higher magnitude. This, in agreement with Eq. (1), does not give rise to sensitivity values due to a smaller magnitude of the current imbalance compared to the total current. However, total current reduces with a faster rate

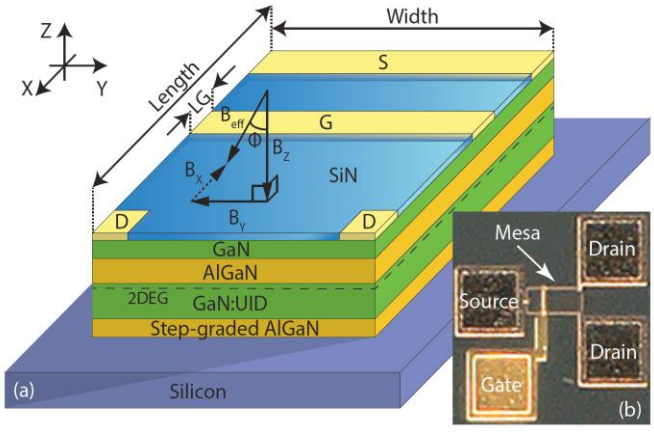

Figure 1. (a) Three-dimensional schematic of dual-drain GaN MagHEMT showing device (not to scale) on silicon substrate and its magnetic field components resulting from the magnetic concentration where Φ is the angle between the magnetic field Bz applied perpendicular to surface and effective magnetic field B_{eff}. (b) Micro-photograph of a fabricated GaN MagHEMT and its contact pads.

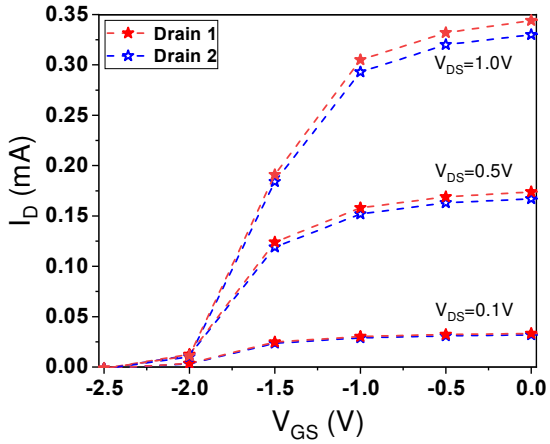

Figure 2. Measured transfer characteristics of dual drain GaN MagHEMT at room temperature with gate length of L_G=5 µm, device length of L=65 µm and device width of W=20 µm at various drain biases in the absence of magnetic field.

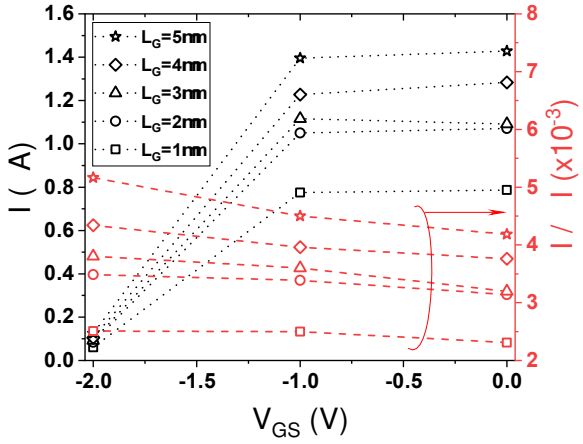

Figure 3. Measured mean current imbalance (ΔI) and its ratio to total current (ΣI=I_{D1}+I_{D2}) in dual-drain GaN MagHEMTs at room temperature with device length of L=65 µm, device width of W=20 µm and gate to source spacing of L_{GS}=7 µm for different gate length of L_G=1 µm (squares), L_G=2 µm (circles), L_G=3 µm (triangles), L_G=4 µm (diamonds) and L_G=5 µm (stars) at V_{DS}=0.5V and B=30 mT.

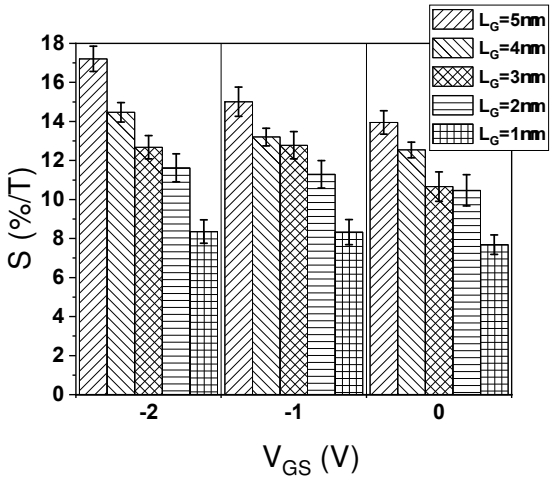

Figure 4. Mean sensitivity of 10 fabricated GaN MagHEMTs at room temperature with gate to source spacing of L_{GS}=7 µm and different gate lengths of L_G=1µm to L_G=5µm with their standard deviations (bars) measured at V_{DS}=0.5V under a magnetic field of B=30 mT applied perpendicular to the device surface. Device length and width are kept constant at L=65 µm and W=20 µm, respectively.

compared to current difference as a function of the input voltage making the ratio (ΔI/ΣI) larger when close to the pinch-off.

The change in lateral electric field with respect to gate to drain spacing of GaN HEMTs has been reported in details in [19]. Since the GaN MagHEMTs operate at a low drain to source voltage, the lateral electric field in the channel is much lower than that required for velocity saturation (125 kV/cm) [20]. Therefore, the electron velocity should be proportional to the lateral electric field as v=$\mu_{channel}E_{lateral}$. By increasing the lateral electric field and therefore average electron velocity, one may manipulate the Lorentz force experienced by the carriers in the 2DEG channel. This will enhance carrier deflection in the presence of magnetic field seen in Figure 3. Hence, improvement in sensitivity for increased gate lengths is observed in Figure 4. The sensitivity of 17.21 %/T is achieved at V_{GS}=–2V for a MagHEMT with gate length of L_G=5 µm.

It is expected that the sensitivity degrades at high temperatures due to increase in Schottky gate leakage currents [21]. Thus, improving the gate to sustain high sensitivities at elevated temperatures is required using metal insulator semiconductor (MIS)-gates in future works.

In what follows, we report on a novel magnetic flux concentrator designed for long MagHEMTs and their specific dimensions with a length of L=65 µm and a width of W=20 µm. The development is necessary to fully understand the requirement for successfully monolithic integration of the magnetic sensors with a SenseFET to achieve galvanic SenseHEMT.

III. Study of Single and Spiral On-chip Concentrators

Figures 5 (a) and 5 (b) are top and side view of the single loop magnetic flux concentrator, respectively, proposed in [15] for 15µm×15µm active device area. The magnetic field in this zigzag shaped magnetic film penetrates the substrate at the points of discontinuity, marked B and C in Figure 5 (b), converting the horizontal field to the vertical one [15]. The magnetic field at the surface of sensor in the normal direction can be related to the current through loop by:

$$B_H = F_I G_M I_0 \tag{3}$$

where F_I is the conversion factor in the absence of the flux concentrator, G_M is the magnetic gain depending on the shape and the magnetic properties of the flux concentrator and I_0 is the current flowing through the metal strip.

The F_I depends upon the relative position of the sensor and the copper loop, and the width and length of the current loop. Based on a current carrying capability of Cu/Au of 10^6 A/cm^2 [22], current range of up to 100 mA can be safely designed using line area of W_{Cu}×t_{Cu}=2×1 µm^2 (where W_{Cu} is the width and t_{Cu} is the thickness of the copper).

The effective conversion factor of the structure can be defined as F_c:

$$F_c = F_I G_M \tag{4}$$

The relationship between sensitivity (S), its current deflection (ΔI), flowing current (I_0) to be sensed (from metal strip) and conversion factor can be expressed by:

$$\frac{\Delta I}{\Sigma I} = \frac{F_c\, S\, I_0}{100\%} \tag{5}$$

where ΣI is the total currents from drain 1 and drain 2 in the presence of magnetic field.

The long and narrow silicon MagFETs and GaN MagHEMTs have demonstrated improved sensitivities [11], [17], [23] as the optimum length to width ratio (L/W) enhances the geometrical correction factor (G_H) holding a linear

relationship with sensitivity [23]. In sensitivity calculations, the correction factor term takes into account the field distribution that is influenced by the non-ideality of sense contacts [17]. However, the conversion factor, F_c, of the single loop concentrator presented in Figures 5 (a) and 5 (b) degrades quickly along the long MagHEMTs. Therefore, an alternative design is required for successful integration.

A copper spiral concentrator shown in Figures 5 (c) and 5 (d) is proposed and investigated for the long current transducer presented in Figure 1.

The magnetic concentrator is evaluated in ANSYS Maxwell [24]. The thickness of the SiN dielectric is 300 nm sandwiched between the copper and the 200nm magnetic film. The relative permittivity of SiN is set to ε_r=7 and the relative permeability of the magnetic film is chosen as μ_r=1000 (similar to CoTaZr) [25]. The thickness (t_{Cu}) and width (W_{Cu}) of the copper metal in the loop are set to 1 µm and 2 µm, respectively.

The magnetic field induced by the flux concentrator (B_{eff}) is at an angle, Φ with respect to its z-component labelled (B_z) in Figure 1 (a). The contours of Φ and B_z in the single loop configuration of the flux concentrator presented in Figures 5 (a) and (b) are plotted in Figures 6 (a) and (b), respectively. The Φ remains less than 1° for nearly 90% of the sensor surface and less than 5° throughout the rest. Such a small deviation cannot be obtained from concentrators which rely on fringing magnetic fields, such as tip concentrators and IMCs, unless their size is several orders larger than the sensor. The magnitude of the field increases by 3-4 times as moved towards the edge (see Figure 6 (b)). Hence the conversion factor defined by (3) and (4) as the ratio of the magnetic field to the current flowing through the loop is higher at the edge compared to the centre of single loop flux concentrator.

The conversion factor and inductance of the single loop structure (along LL in Figure 5 (a)) is plotted in Figure 7 (squares). The conversion factor reduces from 96 mT/A for a L×W=15×15 µm² active device area in [15] to 58 mT/A as the length increases and the magnetic field reduces due to the increase in separation of the current paths.

To improve the conversion factor, a second copper loop in the spiral shape is designed (see Figures 5 (c) and (d)) as two

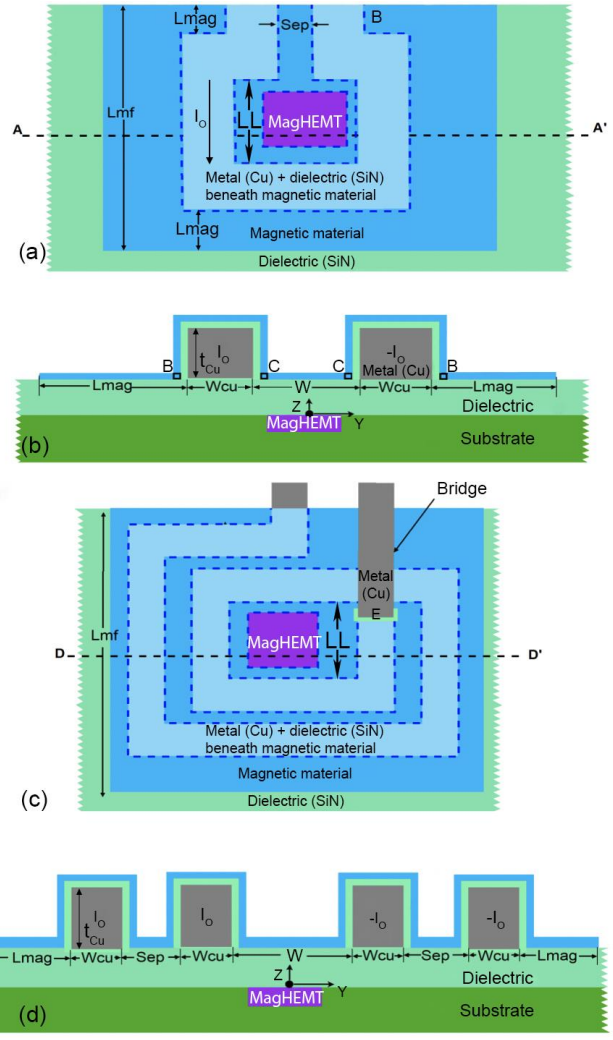

Figure 5. (a) Top view of the single loop flux concentrator with dimensions of 15×15 µm², (b) its cross-sectional view at A-A', (c) top view of the spiral flux concentrator with dimensions > 15×15 µm² and (d) its cross-sectional view at D-D'.

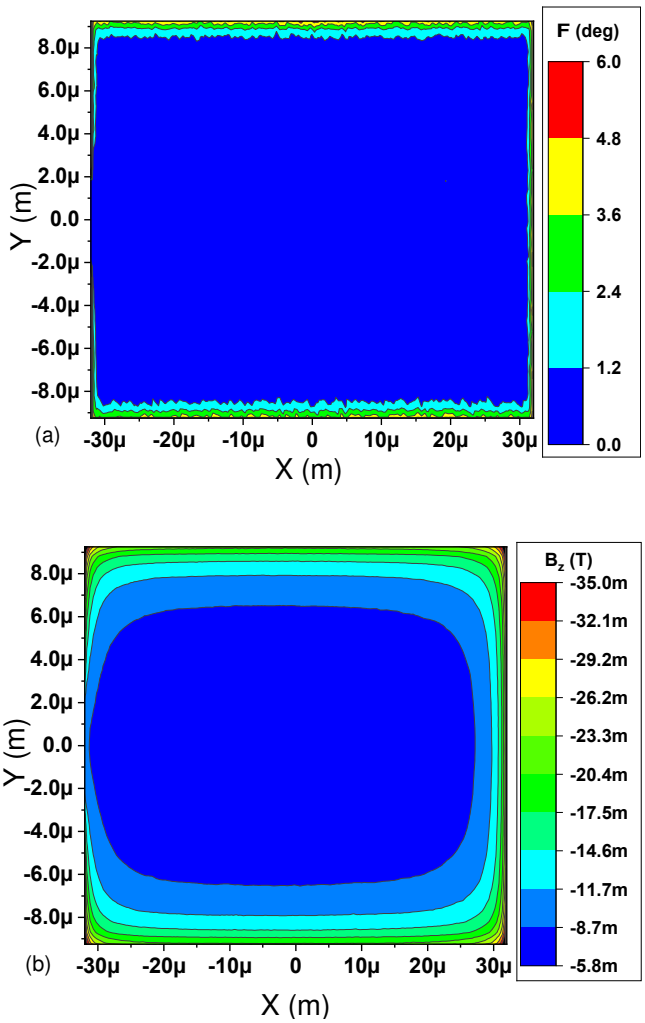

Figure 6. Contours of (a) Φ, angle between the B_Z and effective magnetic field (B_{eff}), (b) strength of magnetic field (B_Z) along z-direction above the sensor for a single loop flux concentrator.

loops in a planar geometry do not improve the performance (simulations are not presented here). The predicted conversion factor of F_C=96 mT/A for spiral magnetic flux concentrator is shown in Figure 7 (circles). The improved conversion factor comes at the price of increased inductance (see Figure 7). However, the values are less than 1 nH and therefore a minimal impact on the rise time is expected.

In contrast to a single loop design in which length (LL) can be chosen as same as the sensor, the spiral flux concentrator needs to be longer than the sensor. This is because, at the air bridge (marked 'E' in Figure 5 (c)), the flow of current lies along the *z*- direction and the fringing fields from the discontinuity of the magnetic film at 'E' contribute to the magnetic fields along X and Y directions, i.e. tangential to the surface of the sensor. This effect is illustrated by modelling the contours of Φ, angle btween B_z and B_{eff}, at the surface of the sensor and presenetd in Figure 8. The direction of the fringing field is no longer in the *z*-direction near point 'E', but remains as high as 60°, in comparison to 6° in the centre. As a result, the double or multiloop structure is at least 15 µm longer in the present case.

The proximity of the current loop to the sensor is limited by the quality of the SiN dielectric, and its thickness. The conversion factor as a function of the distance between the flux concentrator and the MagHEMT is plotted in Figure 9. The thickness of the SiN can be increased up to 2 µm without significant degradation in the conversion factor. Additionally, F_C remains above ~79.5 mT/A (~94% of the maximum value) even at the dielectric thickness of 4 µm.

A comparison between the predicted conversion factors, F_C, measured sensitivities, S, and their products with literature is presented in Table I. Results of this paper show significant improvement compared to the values reported previously [26], [27].

IV. Conclusion

This work highlights key requirements of high performance GaN MagHEMT sensors for protection of high frequency power converters. GaN MagHEMTs of different gate lengths are presented under various biasing conditions at room temperature. The current sensors show improved sensitivities as a result of optimised geometrical factors. Three-dimensional simulations are carried out to investigate the conversion factor of a magnetic flux concentrator designed for integration with the GaN MagHEMTs using ANSYS. A reduction in the conversion factor by 50 % is predicted from the single loop design for long MagHEMTs. Therefore, a spiral magnetic flux concentrator is proposed. The product of conversion factor (85 mT/A) from the new configuration and the measured GaN MagHEMT sensitivity (17.21 %/T) suggests the detection of currents almost three times (3×) smaller than the CMOS metal line structure.

TABLE I: A COMPARISON OF THE F_C, S AND F_C*S FROM THIS WORK WITH LITERATURE.

Ref.	Technology	Structure	Predicted F_C (mT/A)	Measured S (%/T)	Predicted F_C*S (%/A)
[26]	Si-CMOS	On-chip Metal line	4.95	--	--
[27]	Si-CMOS	On-chip Metal line	8	2.6	0.021
This work	GaN	Single Loop	58	17.21	0.998
This work	GaN	Spiral Loop	85	17.21	1.46

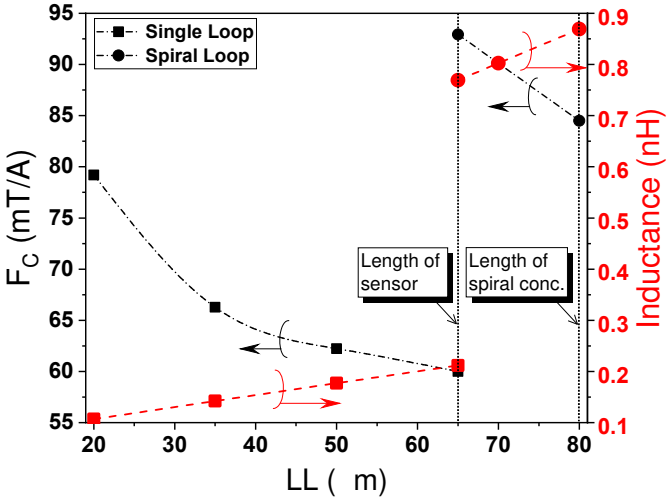

Figure 7. Conversion factor and inductance of the single loop (squares) and spiral (circles) magnetic flux concentrators predicted in ANSYS using the SiN thickness of 300 nm with the relative permittivity of ε_r=7 sandwiched between the copper and the 200nm magnetic film with the relative permeability of μ_r=1000.

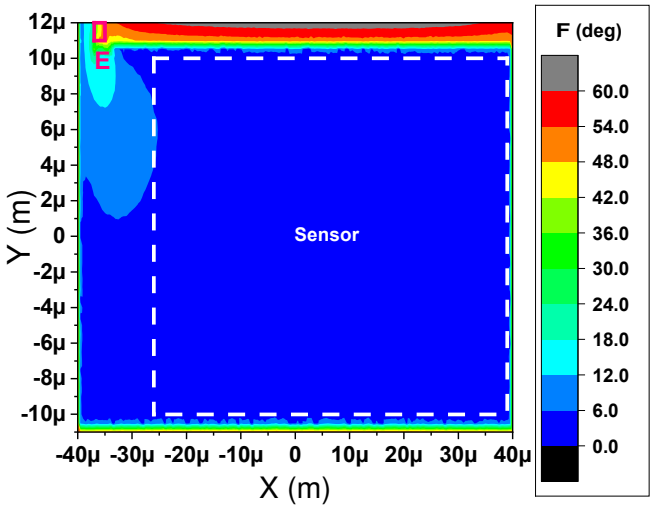

Figure 8. Contours of the Φ, angle between the B_Z and effective magnetic field (B_{eff}) above the sensor, for the spiral flux concentrator predicting an angular deviation less than 6 degrees in centre.

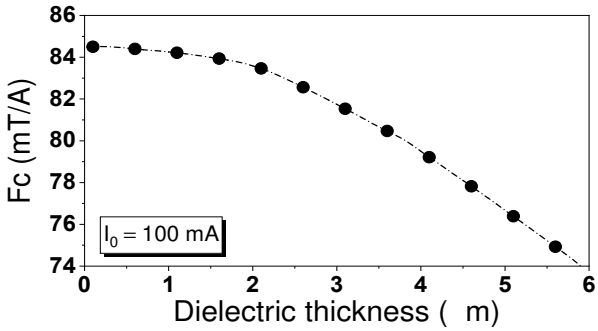

Figure 9. Predicted conversion factor as the function of distance between the spiral flux concentrator and the MagHEMT with the current of 100 mA flowing through its metal strip.

REFERENCES

[1] S. J. Nibir, M. Biglarbegian, and B. Parkhideh, "Performance study of magnetic field concentration techniques on magnetoresistor/Rogowski contactless current sensor", *IEEE Sensors*, pp. 1-3, Jan. 2017. doi: 10.1109/ICSENS.2016.7808725

[2] S. Ziegler, R. C. Woodward, H. H.-C. Iu, and L. J. Borle, "Current sensing techniques: a review", *IEEE Sens. J.*, vol. 9, no. 4, pp. 354–376, Apr. 2009. doi: 10.1109/JSEN.2009.2013914

[3] A. Patel and M. Ferdowsi, "Current sensing for automotive electronic-a survey", *IEEE Trans. Veh. Technol.*, vol. 58, no. 8, pp. 4108–4119, May 2009. doi: 10.1109/TVT.2009.2022081

[4] M. H. Alvi, M. Sheng, R. Lorenz, "2-D magnetoresistive point field detector-based current sensing for high-density power modules", *IEEE Appl. Power Electron. Conf. and Expo.*, pp. 633-639, May 2019. doi: 10.1109/APEC.2019.8721938

[5] E. Ramsden, "Hall-effect sensors: theory and applications", 2nd ed., Elsevier: Burlington, MA, USA, 2006.

[6] A. C. Beer, "The Hall effect and related phenomena", *Solid State Electron.*, vol 9, no. 5, pp. 339-351, May 1966. doi: https://doi.org/10.1016/0038-1101(66)90148-1

[7] R. C. Gallagher and W. S. Corak, "A metal-oxide-semiconductor (MOS) Hall element", *Solid. State. Electron.*, vol. 9, no. 5, pp. 571–580, May 1966. doi: https://doi.org/10.1016/0038-1101(66)90172-9

[8] S. Faramehr, K. Kalna, and P. Igić, "Drift-diffusion and hydrodynamic modeling of current collapse in GaN HEMTs for RF power application", *Semicond. Sci. Technol.*, vol. 29, no. 2, pp. 025007-025017, Jan. 2014. doi: https://doi.org/10.1088/0268-1242/29/2/025007

[9] S. Faramehr, K. Kalna, and P. Igić, "Design and simulation of a novel 1400 V–4000 V enhancement mode buried gate GaN HEMT for power applications", *Semicond. Sci. Technol.*, vol. 29, no. 11, pp. 115020-115026, Sep. 2014. doi: https://doi.org/10.1088/0268-1242/29/11/115020

[10] B. R. Thomas, S. Faramehr, D. C. Moody, J, Evans, M. P. Elwin, and P. Igic, "Study of GaN dual-drain magnetic sensor performance at elevated temperatures", *IEEE Trans. Electron Devices*, vol. 66, no. 4, pp. 1937-1941, Apr. 2019. doi: 10.1109/TED.2019.2901203

[11] R. Rodriguez-Torres, E. A. Gutiérrez-Domínguez, R. Klima and S. Selberherr, "Analysis of split-drain MagFETs", *IEEE Trans. Electron Devices*, vol. 52, no. 12, Nov. 2004. doi: 10.1109/TED.2004.839869

[12] H. Ohta, S. W. Kim, S. Kameki, A. Yamamoto, T. Hashizume, "High thermoelectric power factor for high mobility 2d electron gas", *Adv. Sci.,* pp. 1700696 (p6), Nov. 2017. doi: https://doi.org/10.1002/advs.201700696

[13] H. Blanchard, L. Chiesi, R. Racz and R. S. Popovic, "Cylindrical Hall device", *in Proc. IEDM*, pp. 541-544, Aug. 2002. doi: 10.1109/IEDM.1996.554041

[14] P. M. Drljača, F. Vincent, P. A. Besse, and R. S. Popovic, "Design of planar magnetic concentrators for high sensitivity Hall devices", *Sens. Actuators, A.*, vol. 97–98, pp. 10–14, Jan. 2002. doi: https://doi.org/10.1016/S0924-4247(01)00866-4

[15] N. Poluri and M. M. De Souza, "An Integrated On-Chip Flux Concentrator for Galvanic Current Sensing", *IEEE Electron Device Lett.*, vol. 39, no. 11, pp. 1752–1755, Sep. 2018. doi: 10.1109/LED.2018.2868647

[16] R. S. Popovic, "Hall effect devices", 2nd ed., Institute of Physics Publishing, IOP, Bristol and Philadelphia, 2004.

[17] J. W. A. von Kluge and W. A. Langheinrich, "An analytical model of MAGFET sensitivity including secondary effects using a continuous description of the geometric correction factor G," *IEEE Trans. Electron Devices*, vol. 46, no. 1, pp. 89–95, Jan. 1999. doi: 10.1109/16.737446

[18] V. Mosser, N. Matringe and Y. Haddab, "A spinning current circuit for Hall Measurements down to the nanotesla range", *IEEE Trans. Instrum. Meas.,* vol. 66, no. 4, pp. 637-650, Apr. 2017. doi: 10.1109/TIM.2017.2649858

[19] S. Russo and A. Di Carlo, "Influence of the source–gate distance on the AlGaN/GaN HEMT performance", *IEEE Trans. Electron Devices*, vol. 54, no. 5, pp. 1071–1075, May 2007. doi: 10.1109/TED.2007.894614

[20] T. Palacios, S. Rajan, A. Chakraborty, S. Heikman, S. Keller, S. P. DenBaars, and U. K. Mishra, "Influence of dynamic access resistance in g_m and f_T linearity of AlGaN/GaN HEMTs", *IEEE Trans. Electron Devices*, vol. 52, no. 10, pp. 2117-2123, Oct. 2005. doi: 10.1109/TED.2005.856180

[21] C. Unger, M. Mocanu, M. Pfost, P. Waltereit, R. Reiner, "Pulse robustness of AlGaN/GaN HEMTs with Schottky and MIS gates", in *Proc. 29th ISPSD*, pp. 451-454, Jul. 2017. doi: 10.23919/ISPSD.2017.7988915

[22] C. Subramaniam, T. Yamada, K. Kobashi, A. Sekiguchi, D. N. Futaba, M. Yumura, K. Hata, "One hundred fold increase in current carrying capability in carbon nanotune-copper composite", *Nat. Commun.*, vol. 4, p. 2202, Jul. 2013.

[23] S. Faramehr, N. Jankovic, and P. Igic, "Analysis of GaN MagHEMTs", *Semicond. Sci. Technol.*, vol. 33, no. 9, pp. 095015-095022, Aug. 2018. doi: https://doi.org/10.1088/1361-6641/aad58f

[24] ANSYS® Maxwell, RELEASE 18.2

[25] D. S. Gardner, G. Schrom, P. Hazucha, F. Paillet, T. Karnik, and S. Borkar, "Integrated on-chip inductors with magnetic films", *IEEE Trans. Magn.*, vol. 43, no. 6, pp. 2615–2617, Jun. 2007. doi: 10.1109/TMAG.2007.893794

[26] F. C. Castaldo, P. Rodrigues, and C. A. Reis Filho, "Shunt-zero based on CMOS split-drain: A practical approach for current sensing," *IEEE Annu. Power Electron. Spec. Conf.*, vol. 2005, no. 3, pp. 1745–1749, Jan. 2006. doi: 10.1109/PESC.2005.1581866

[27] O. Aiello and F. Fiori, "A new MagFET-based integrated current sensor highly immune to EMI", *Microelectron. Reliab.*, vol. 53, no. 4, pp. 573–581, Apr. 2013. doi: https://doi.org/10.1016/j.microrel.2012.10.013